NEURAL REGENERATION RESEARCH
www.nrronline.org

Research Article

In vivo neuronal and astrocytic activation in somatosensory cortex by acupuncture stimuli

https://doi.org/10.4103/1673-5374.339003
Date of submission: October 27, 2021
Date of decision: November 27, 2021
Date of acceptance: January 19, 2022
Date of web publication: April 1, 2022

Xiao-Yue Chang[1, 2, #], Kai Chen[1, #], Tong Cheng[1, #], Pui To Lai[2], Li Zhang[1, 3, 4, *], Kwok-Fai So[1, 2, 3, 4, 5, *], Edward S. Yang[2, *]

From the Contents

Graphical Abstract *Involvement of both neurons and astrocytes in acupuncture treatment*

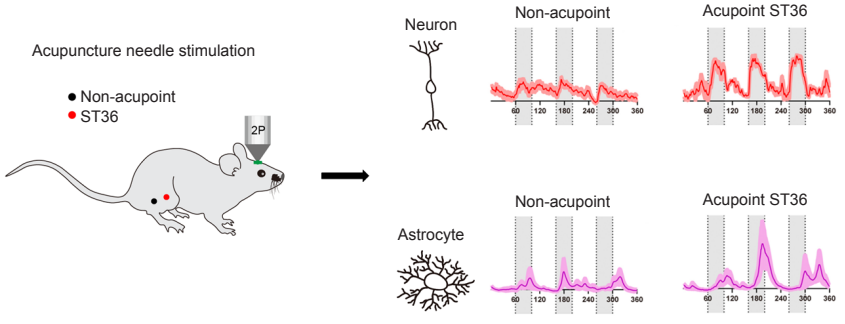

Abstract

Acupuncture is a medical treatment that has been widely practiced in China for over 3000 years, yet the neural mechanisms of acupuncture are not fully understood. We hypothesized that neurons and astrocytes act independently and synergistically under acupuncture stimulation. To investigate this, we used two-photon *in vivo* calcium recording to observe the effects of acupuncture stimulation at ST36 (*Zusanli*) in mice. Acupuncture stimulation in peripheral acupoints potentiated calcium signals of pyramidal neurons and astrocytes in the somatosensory cortex and resulted in late-onset calcium transients in astrocytes. Chemogenetic inhibition of neurons augmented the astrocytic activity. These findings suggest that acupuncture activates neuronal and astrocytic activity in the somatosensory cortex and provide evidence for the involvement of both neurons and astrocytes in acupuncture treatment.

Key Words: acupuncture; astrocyte; chemogenetic; neuron; N-methyl-D-aspartate receptor; somatosensory cortex; transient receptor potential A1; two-photon *in vivo* imaging

Introduction

Acupuncture is a technique that has been practiced for millennia (Linde et al., 2005; Witt et al., 2005; Haake et al., 2007; Walker et al., 2010). The clinical benefit of acupuncture for pain management has been recognized by accumulating clinical evidence (Witt et al., 2005; Hinman et al., 2014; Jensen and Finnerup, 2014; Scarborough and Smith, 2018). Although the practice is currently used worldwide, its mechanism is unknown. Previous studies in mouse models have demonstrated that the release of neuromodulators adenosine triphosphate and dopamine, mediated by ascending and vagus nerves, plays a role in anti-nociceptive and anti-inflammatory actions of acupuncture (Goldman et al., 2010; Torres-Rosas et al., 2014; Park and Namgung, 2018). It remains unknown whether neurons or astrocytes play the central role in the neural mechanism of acupuncture, or whether they work together to achieve the therapeutic effect.

The primary somatosensory cortex (S1) processes both spatial and graded pain information (Bushnell et al., 1999; Aronoff et al., 2010). A recent study suggested that S1 plays a role in the top-down modulation of nociceptive inputs from the spinal cord (Liu et al., 2018). Human imaging data has suggested the rewiring of somatosensory cortex after acupuncture (Maeda et al., 2017); however, *in vivo* and real-time neural activity during the course of acupuncture has not been demonstrated at the single-cell level.

We hypothesized that the brain and the central nervous system, in particular, neurons and astrocytes, are actively engaged both independently and cooperatively in response to acupuncture stimuli. In the present study, we investigated the hypothesis by imaging *in vivo* cellular activity in somatosensory cortex of mice during acupuncture. The objective of this study was to investigate the fundamental mechanism of acupuncture to determine if there is a cellular foundation.

Materials and Methods

Animals

Male C57BL/6J mice (n = 60, 4 weeks old, specific pathogen-free) were purchased from Guangdong Medical Laboratory Animal Center (license No. SCXK(Yue)2019-0035). Mice were group-housed under a 12-hour light/dark cycle and were provided with water and food ad libitum. All experimental protocols were preapproved by the Ethics Committee of Experimental Animals of Jinan University (approval No. 2019393) on February 27, 2019 in accordance with Institutional Animal Care and Use Committee guidelines for animal research. All experiments were designed and reported according to the Animal Research: Reporting of *In Vivo* Experiments (ARRIVE) guidelines (Percie du Sert et al., 2020).

Stereotaxic viral injection

In this experiment, the following adeno-associated virus (AAV) vectors were administered: AAV-hsyn-GCaMP6s (150 nL per site without dilution, titer: > 1×10^{13} genome copies per mL) for neuronal calcium activity recording; AAV-gfaABC1D-lck-GCaMP6f (250 nL per site without dilution, titer: 1.2×10^{13} genome copies per mL) for astrocytic calcium activity recording, and a 2:1 mixture of AAV-gfaABC1D-lck-GCaMP6f and AAV-CaMKIIa-hM4D(Gi)-mCherry

[1]Key Laboratory of CNS Regeneration (Minstry of Education), Guangdong-Hong Kong-Macau Institute of CNS Regeneration, Jinan University, Guangzhou, Guangdong Province, China; [2]Department of Electrical and Electronic Engineering, The University of Hong Kong, Hong Kong Special Administrative Region, China; [3]Center for Brain Science and Brain-Inspired Intelligence, Guangdong-Hong Kong-Macao Greater Bay Area, Guangzhou, Guangdong Province, China; [4]Guangzhou Regenerative Medicine and Health Guangdong Laboratory, Guangzhou, Guangdong Province, China; [5]State Key Laboratory of Brain and Cognitive Science, Li Ka Shing Faculty of Medicine, The University of Hong Kong, Hong Kong Special Administrative Region, China

***Correspondence to:** Li Zhang, PhD, zhangli@jnu.edu.cn; Kwok-Fai So, PhD, hrmaskf@hku.hk; Edward S. Yang, PhD, esyang123@hotmail.com.
https://orcid.org/0000-0003-1489-0879 (Li Zhang); https://orcid.org/0000-0003-4039-4246 (Kwok-Fai So)
#These authors contributed equally to this work.

Funding: *This study was supported by National Key Research and Development Program of China, No. 2016YFC1306702 (to KFS and LZ); the National Natural Science Foundation of China, No. 81771455 (to KFS); Science and Technology Program of Guangdong Province of China, No. 2018B030334001 (to KFS); and the Natural Science Foundation of Guangdong of China, No. 2019A1515011772 (to LZ).*

How to cite this article: *Chang XY, Chen K, Cheng T, Lai PT, Zhang L, So KF, Yang ES (2022) In vivo neuronal and astrocytic activation in somatosensory cortex by acupuncture stimuli. Neural Regen Res 17(11):2526-2529.*

(350 nL per site, titer: 5.7E+12 vector genomes per mL) for chemogenetic inhibition of calcium/calmodulin-dependent protein kinase II (CaMKII) neurons. All viral vectors were purchased from Taitool Bioscience, Shanghai, China.

For viral transfection, mice were anesthetized with an intraperitoneal injection of 1.25% Avertin (Sigma-Aldrich, St. Louis, MO, USA). A scalp incision was made with eye scissors after local sterilization, and a hole was made in the skull with a high-speed microdrill to provide access to the primary somatosensory cortex (0.02 mm posterior and 1.5 mm lateral from Bregma) (Rosenthal et al., 2021). A glass micropipette connected to an ultra-micro injection pump (WPI, Sarasota, FL, USA, Nanoliter2010) was used to inject virus into the designated area. After each injection, the micropipette was held in place for 10 minutes before being retracted to ensure adequate viral delivery. The head incision was then closed and the mouse was returned to its cage. After the surgery, mice were allowed a 3-week recovery before the calcium recordings (**Figure 1**).

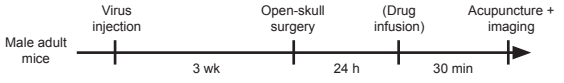

Figure 1 | **Study flowchart.**

In vivo two-photon imaging

In vivo two-photon imaging was performed as previously described (Holtmaat et al., 2009). To record calcium activity in the sensory cortex of awake mice, the mouse head was fixed onto a solid metal plate using a customized scaffold that was fixed on the skull using dental cements. S1 was localized (0.5 mm anterior and 1.5 mm lateral to the Bregma) using a stereotaxic apparatus (RWD, Shenzhen, China). The scalp and skull covering the sensory cortex were removed to create an imaging window (2 mm radius), which was covered with a glass coverslip. The imaging session was performed at 24 hours after the craniotomy surgery. The mouse received acupuncture needle stimulation (as described below) under a two-photon microscope (Zeiss, Jena, Germany, LSM780) with a 20× water immersion objective using a 920 nm laser for green fluorescent-calmodulin proteins (GCaMPs) excitation. The calcium signals were captured from neurons and astrocytes in layer V (500 to 600 μm below the pia), using a frame rate at 2 Hz with 4× digital zoom, 0.75 μm interval, 512 × 512 pixels.

Acquired images were corrected for spatial distortions using the TurboReg package of ImageJ v1.52a (National Institutes of Health, Bethesda, MD, USA) (Schneider et al., 2012). Time-series images were processed in ImageJ to manually delineate regions of interest, from which the mean intensity of calcium values (F) was extracted. Data were then normalized as $\Delta F/F_0$ with the calculation $(F - F_0)/F_0$, where F_0 (basal value) was the averaged F values during the first 30 seconds of each recording session. A calcium transient was defined as when the $\Delta F/F_0$ value exceeded the basal level by at least three folds of standard deviation of population $\Delta F/F_0$. The total integrated calcium was calculated as the time-integration of all $\Delta F/F_0$ values during the recording period. In some recording sessions, clozapine-N-oxide (2 mg/kg, Abcam, Cambridge, UK) was applied via intraperitoneal injection at 30 minutes before Ca^{2+} imaging (and acupuncture stimulation). MK801 (N-methyl-D-aspartate receptor (NMDAR) antagonist; 0.1 mg/kg, MedChem Express, Princeton, NJ, USA) or HC030031 (A1 cation channel receptor antagonist; 25 mg/kg, Sigma-Aldrich) was applied directly onto the dura matter via the transcranial imaging window.

Manual acupuncture stimulation

Acupuncture stimulation was performed during all calcium imaging sessions. We chose ST36 (*Zusanli*) as the major stimulation acupoint as it is widely used in relieving neuropathic pain (Kim et al., 2018). ST36 is located 4 mm below and 1–2 mm lateral to the midpoint of the knee in mice. A second acupoint, GB34 (*Yanglingquan*) located at the depression anterior and inferior to the fibular head was also used. The non-acupoint control site was located 2 mm outside of the ST36. An acupuncture needle (0.35 mm × 25 mm, Hwato, Suzhou, China) was slowly inserted vertically into the acupoint with a depth of 2 mm. Acute acupuncture recording sessions lasted for 3 minutes, during which three consecutive acupuncture sessions (20-second duration for each, with the needle twisted twice per second) were applied with a 30-second interval between the two sessions. For chronic recordings, 20-minute persistent needle stimulation was performed.

Immunofluorescence staining

After calcium imaging, mice were intraperitoneally anesthetized using 1.25% Avertin and perfused with 4% paraformaldehyde. The whole brain tissue was immersed in 4% paraformaldehyde overnight, and was then dehydrated with 30% sucrose. The brain tissues were sectioned into coronal slices (40 μm thickness) using a sliding microtome (Leica, Wetzlar, Germany). Brain slices were washed in phosphate buffered saline and were blocked for 2 hours in 2% bovine serum albumin. The primary antibodies (mouse anti-mouse NeuN, 1:500, Synaptic Systems, Goettingen, Germany, Cat# 266011, RRID: AB_2713971; rabbit anti-mouse Neurogranin, 1:500, Millipore, Temecula, CA, USA, Cat# AB5620, RRID: AB_91937; mouse anti-mouse Parvalbumin (PV), 1:500, Millipore, Cat# MAB1572, RRID: AB_2174013; rabbit anti-mouse S100b, 1:500, Sigma-Aldrich, Cat# HPA015768, RRID: AB_1856538; rabbit anti-mouse ionized calcium binding adaptor molecule 1 (Iba-1), 1:1000, Wako, Richmond, VA, USA, Cat# 019-19741, RRID: AB_839504; rabbit anti-mouse oligodendrocyte transcription factor 2 (Olig2), 1:500, Abcam, Cat#ab109186, RRID: AB_10861310; rabbit anti-mouse c-fos, 1:1000, Cell Signaling Technology, Danvers, MA, USA, Cat# 2250S, RRID: AB_2247211) diluted in blocking solution were applied to the slices and incubated at 4°C for 48 hours. After phosphate buffered saline washes, slices were then incubated with the appropriate fluorophore-conjugated secondary antibody (goat anti-mouse conjugated Alexa Fluor 594, 1:500, Jackson ImmunoResearch, West Grove, PA, USA, Cat# 115-587-003, RRID: AB_2338900; donkey anti-rabbit conjugated with Alexa Fluor 594, 1:500, Jackson ImmunoResearch, Cat# 711-585-152, RRID: AB_2340621) for 2 hours at room temperature. Images were captured using a confocal microscope (ZEISS).

Statistical analysis

All data were presented as mean ± standard error of mean (SEM). All data were analyzed using GraphPad Prism 6.0 (GraphPad Software, San Diego, CA, USA, www.graphpad.com). Parametric data were compared using one-way analysis of variance followed by Bonferroni's multiple comparison tests. Non-parametric data were analyzed by Mann-Whitney *U* test.

Results

Acupuncture induces calcium transients in S1 neurons

We used two-photon microscopy in mice transfected with an AAV vector expressing fluorescent calcium indicator GCaMP6s (**Additional Figure 1**), and recorded the calcium activity of layer 5 pyramidal neurons (L5PNs) while the mouse received manual acupuncture stimulation at the hindlimb acupoint ST36 or GB34 (**Figure 2A**).

For each mouse, we compared calcium activity within the same field of view under different scenarios: non-acupoint stimulus on the contralateral side of field of view; puncture at ST36 on contralateral side or ipsilateral side; or ST36 puncture under general anesthesia (**Figure 2B**). Compared with the non-acupoint control, stimulation at ST36 on the contralateral side remarkably activated calcium transients, which were synchronized with each acupuncture course (**Figure 2C** and **D**, with gray shades). Acupuncture at ST36 on the ipsilateral side also induced calcium activation of L5PNs, but with lower intensity compared with that induced by contralateral side puncture (**Figure 2E**). The induced calcium potentiation in S1 was silenced on each side by general anesthesia (**Figure 2F** and **G**) and was not observed in the primary motor cortex (M1; **Figure 2H** and **I**). These results indicate that S1 activation was induced by acupuncture stimulation, and did not represent artifacts such as from body movements. Needle stimulation at a second acupoint (GB34) also led to higher neuronal calcium activity compared with that at the non-acupoint control (**Figure 2J**). Furthermore, the calcium potentiation was largely abolished by the pre-infusion of MK801, which is a potent antagonist for NMDAR, suggesting that the induced calcium activity was mainly dependent on glutamatergic transmission (**Figure 2K** and **L**).

Acupuncture activates calcium transients in astrocytes

We next investigated whether acupuncture stimulation affects astrocytes. Recent *in vivo* studies have suggested that neuronal excitation may alter the calcium signals in astrocytes (Stobart et al., 2018), and that astrocytic activity affects synaptic transmission (Brancaccio et al., 2017). To monitor *in vivo* activity of astrocytes, mice were transfected with GCaMP6f into S1 under a glial fibrillary acidic protein promoter (gfaABC1D) (**Figure 3A**) with astrocyte-preferential expression (**Additional Figure 2**) (Yu et al., 2020). Using two-photon calcium recording, we compared the activity of astrocytes between non-acupoint stimulation and ST36 acupuncture (**Figure 3B**). Consistent with the findings in neurons, acupuncture treatment led to stronger calcium transients in astrocytes compared with non-acupoint stimulation (**Figure 3C** and **D**). The astrocytic calcium signals were remarkably suppressed after MK801 application (**Figure 3E** and **G**), suggesting its dependence on glutamatergic transmission. To further clarify the mechanism, we administered HC030031 to S1 during the *in vivo* recording to block the transient receptor potential A1 cation channel, which is the major calcium transporter in astrocytes (Shigetomi et al., 2011). The application of HC03001 remarkably abolished the astrocytic calcium activity after ST36 acupuncture (**Figure 3F** and **G**). These data collectively suggested the potentiation of astrocytic calcium activity by acupuncture.

Astrocytic calcium activity is mediated by neurons

The abolishment of astrocytic calcium activity by NMDAR blockade (**Figure 3E**) suggested that neuronal activation might be the driving force of astrocytic calcium transients. We then compared the kinetics of calcium spikes between neurons and astrocytes under identical acupuncture treatment. Astrocytic calcium transients showed a slow-onset pattern. Specifically, the neuronal calcium spikes developed immediately after applying the acupuncture (**Figure 2D**), whereas astrocytic calcium transients began to rise at approximately 10–15 seconds after the treatment initiation (**Figure 3D**). The latencies of both the initiation and zenith of astrocytic calcium spikes were over 10 seconds longer than those in neurons (**Figure 3H**). The differential time latency suggested a possible regulatory role of neuronal excitation in driving astrocytic calcium activity.

To investigate this, we transfected inhibitory designer receptors exclusively activated by designer drugs hM4Di into S1 L5PNs, along with the transfection of GCaMP6s into astrocytes (**Figure 4A**). After clozapine-N-oxide administration, PN activity was remarkably suppressed (**Figure 4B**). We next recorded the calcium activity of astrocytes upon acupuncture stimulation.

Clozapine-N-oxide treatment induced a stronger calcium response compared with the response in the saline control group (**Figure 4C** and **D**). These results seemed to indicate: (1) the rise of neuronal and astrocytic calcium transients upon acupuncture is independently regulated; and (2) neuronal activation probably promotes the decay of the astrocytic calcium response, rather than the presumed potentiation role.

Next, we performed a persistent acupuncture treatment to further examine the kinetics of both neuronal and astrocytic calcium activity. Compared with the spontaneous activity under resting state, the 20-minute acupuncture stimulation induced a tonic-like excitation of calcium activity in neurons (**Figure 4E**). In astrocytes, the major calcium peak occurred shortly after the onset of acupuncture followed by multiple lower peaks (**Figure 4F**).

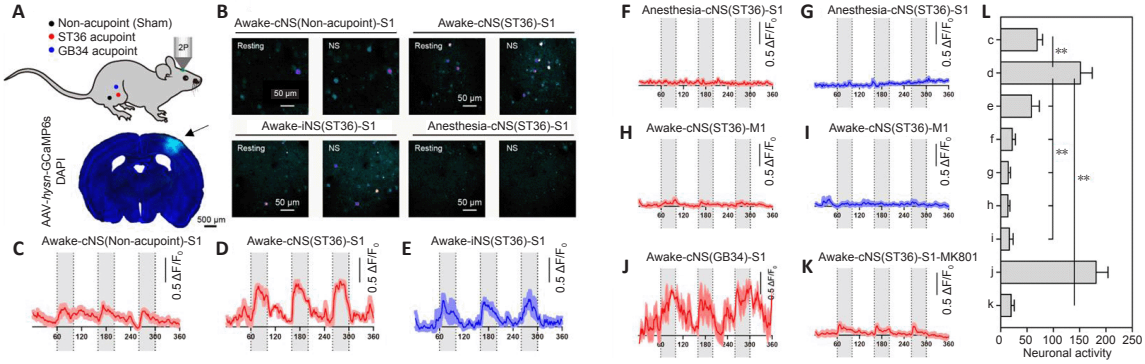

Figure 2 | **Acupuncture induces calcium transients in S1 neurons.**
(A) Top, schematic diagram showing the acupoints ST36 (*Zusanli*) and GB34 (*Yanglingquan*), and non-acupoint in adjacent sites as the sham control group; bottom, transfection sites (arrow) of GCaMP6s in S1. Scale bar: 500 μm. (B) Pseudo-colored images reflecting calcium intensity of neurons in selected field of view from S1 under resting state and during acupuncture. Scale bar: 50 μm. (C–K) Time-series records of normalized calcium values (in $\Delta F/F_0$) during the period of repeated acupuncture stimuli (grey shaded box). The temporal scale (*x*-axis) was presented in seconds. Three acupuncture courses (20 seconds each) were sequentially applied, with a 30-second resting interval between two treatments. In each group, calcium activities from representative fields of view were normalized and averaged for plotting. Fields of view numbers: $n = 10$ for C; $n = 8$ for D, K; $n = 3$ for E–G, J; $n = 6$ for H–I. Animal numbers: $n = 3$ each. (L) Comparison of total integrated neuronal calcium activity during the acupuncture course. Data are expressed as mean ± SEM and were analyzed by one-way analysis of variance. Group effect: $F_{(8, 41)} = 20.10$, $P < 0.001$, Bonferroni's multiple comparison test: $^{**}P < 0.01$. cNS: Needle stimulation on the contralateral side; GCaMP6s: green fluorescent-calmodulin protein 6s; iNS: needle stimulation on the ipsilateral side; M1: primary motor cortex; NS: needle stimulation; S1: primary somatosensory cortex.

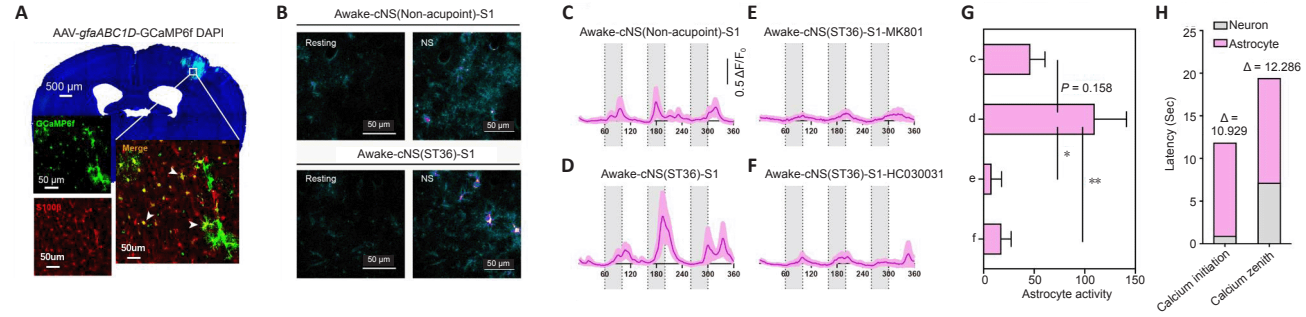

Figure 3 | **Acupuncture activates calcium transients in astrocytes.**
(A) Transfection sites of AAV-gfaABC1D-GCaMP6f in S1 were colocalized with astrocyte marker S100β (white arrowheads, red, stained by Alexa Fluor 594). Scale bars: 50 μm. (B) Pseudo-colored images for the intensity of astrocytic calcium spikes in selected fields of view during the resting state and NS. Scale bars: 50 μm. (C–F) Time-series recordings of normalized calcium values (in $\Delta F/F_0$) during the acupuncture sessions (grey shaded box). The temporal scale (x-axis) was presented in seconds. The protocol of acupuncture was the same as in Figure 2. In each group, the calcium activity from different fields of view was recorded for data plotting. Field of view numbers: $n = 9$ for C–D, $n = 5$ for E, $n = 10$ for F. Animal numbers: $n = 3$ each. (G) Comparison of total integrated astrocytic calcium activity. Data are expressed as mean ± SEM and were analyzed by one-way analysis of variance. Group effect: $F_{(3, 29)} = 5.188$, $P = 0.0054$; Bonferroni's multiple comparison test: $^{*}P < 0.05$, $^{**}P < 0.01$. (H) Comparison of kinetics of calcium spikes between neurons and astrocytes from the recordings under cNS stimulation on ST36 of awake mice. cNS: Needle stimulation on the contralateral side; DAPI: 4′,6-diamidino-2-phenylindole; NS: needle stimulation; S1: primary somatosensory cortex.

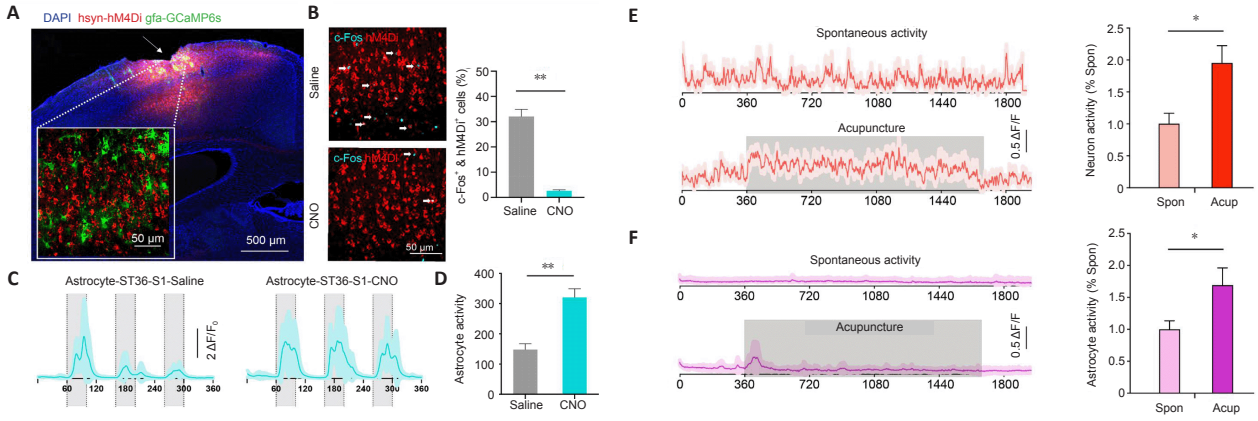

Figure 4 | **Astrocytic calcium activity is mediated by neurons.**
(A) Transfection of hM4Di into excitatory neurons of S1 (arrow) and transfection of gfaABC1D-GCaMP6s into astrocytes. Scale bar: 500 μm. (B) Co-staining (arrows) of c-Fos (blue) and hM4Di (red) in S1. Mice were administered CNO, followed by astrocytic calcium imaging as in C, and were immediately sacrificed for brain sectioning and immunofluorescence assay. Scale bar: 50 μm. Right, CNO treatment significantly suppressed the activity of transfected neurons (Mann-Whitney *U* test, $^{**}P = 0.0012$). (C) Time-series recording of normalized astrocytic calcium signals during acupuncture treatment. Grey shades indicate the acupuncture period. Approximately 15–20 cells from four animals were plotted. (D) Total integrated calcium activity was potentiated by CNO treatment (Mann-Whitney *U* test, $^{**}P = 0.0022$). (E) Left, time-series recordings of normalized neuronal calcium activity under resting state or during 20-minute continuous manual acupuncture on ST36. A total of 18 fields of view (FOVs) from four animals were plotted in each group. Right, the total neuronal calcium activity was elevated under acupuncture (Mann-Whitney *U* test, $^{*}P = 0.0293$). (F) Left, time-series recordings of normalized astrocytic calcium activity under resting state or during the acupuncture on ST36. A total of 18 fields of view from four animals were plotted in each group. Right, the total astrocytic calcium activity was elevated during acupuncture (Mann-Whitney *U* test, $^{*}P = 0.0303$). The temporal scale (*x*-axis) of c–f was presented in seconds. Data are expressed as mean ± SEM. The experiments were repeated twice. Acup: During the acupuncture on ST36; CNO: clozapine-N-oxide; DAPI: 4′,6-diamidino-2-phenylindole; GCaMP6s: green fluorescent-calmodulin protein 6s; S1: primary somatosensory cortex; Spon: resting state.

Discussion

By comparing awake mice with those under anesthesia, the present study provided unambiguous evidence that awake mice exhibited stronger neuronal calcium signaling for both verum acupuncture points (ST36 and GB34) and off-site sham acupuncture. We also performed a similar experiment in which astrocytes in the somatosensory cortex expressed calcium indicator. The present study is the first to show that neurons and astrocytes produced comparable activity under acupuncture stimulation, indicating that acupuncture utilizes both neurons and astrocytes to deliver its sensory effect.

We would like to address a few other interesting findings in the data. First, sham acupoint is not a minor contention, as it has been used to argue for a placebo effect, thus denying the scientific basis not only for sham acupuncture but also for verum acupuncture. Our results are the first to show *in vivo* neuronal and astrocytic communication in response to acupuncture, and to demonstrate that sham acupoint has cellular effects. The results are in agreement with available clinical data (Linde et al., 2005; Witt et al., 2005; Haake et al., 2007). Second, there was strong activity in somatosensory cortex (S1) but no response in motor cortex (M1), indicating the specificity of acupuncture. Third, there was essentially no latency observed in calcium transients in S1 induced by acupuncture at both the sham and acupuncture points, confirming fast neuronal transmission. Fourth, anesthesia inhibited all ST36-S1 responses, indicating the central nervous system has disabled the signaling.

Our findings demonstrated the activation of calcium transients in both cortical neurons and astrocytes during acupuncture stimulation, providing the first *in vivo* and real-time evidence for neural activation induced by acupuncture. Cross-talk exists between these two cell types, and neuronal activation may drive the decay of astrocytic calcium activity. We observed that upon acupuncture stimulation, astrocytes presented a late onset calcium transient, which can be attributed to the gamma-aminobutyric acid-B receptor (Meier et al., 2008). As a result, the brain region-wide inhibition of all neurons may impair the gamma-aminobutyric acid-driven calcium activity, and potentiate the total calcium level.

In addition, astrocytic calcium currents can be initiated independently from neurons. A previous study suggested the activation of adenosine receptors for local anti-nociception during acupuncture stimulation (Goldman et al., 2010). Because of the prominent distribution of adenosine receptors on the astrocyte membrane (Orr et al., 2015; Martin-Fernandez et al., 2017), it is possible that adenosine receptors mediate the acupuncture-induced calcium transients in astrocytes. This mechanism may be related to the pain-relieving function of acupuncture treatment, as one mouse study demonstrated the dependence of electroacupuncture-mediated analgesia on the activation of the adenosine pathway (Liao et al., 2017). It is also interesting to note that elevated S1 activity has been associated with chronic neuropathic pain disorders (Cichon et al., 2017). However, our mechanical acupuncture induced both neuronal and astrocytic activity. These seemingly paradoxical phenomena can be explained by the discrepancy of acute and chronic effects. It is not uncommon to observe long-term depression of synaptic transmission after repeated excitation. We thus speculate that the acute activation of neurons and astrocytes may produce chronically inhibitory effects, probably via neuromodulators that are produced in an activity-dependent manner, such as endorphin or endocannabinoid. These phenomena indicated one possibility that the tonic activation of neurons might cross-talk with astrocytes to relieve them from high-calcium transients. This working model fit with the chemogenetic assay, in which the silencing of neurons led to impaired decay of astrocytic calcium transients, resulting in consecutive high-calcium peaks even after the first acupuncture session. Future studies should be performed to investigate the role of the adenosine receptor pathway. Together, the present findings provide evidence for a dual role of acupuncture in mediating both neuronal and astrocytic activity in cortical regions.

There are some limitations in this study. We focused on acupoint ST36 and somatosensory cortex in mice. To better understand the fundamental neural mechanisms of acupuncture, we confined our research in relation to pain relief. We have not covered other parts of the central nervous system.

In summary, we report that mechanical acupuncture evoked region-specific cortical and NMDAR-dependent neuronal and transient receptor potential A1-dependent astrocytic activity. Chemogenetic-suppressed neuronal influence appeared to enhance astrocytic calcium signaling, a finding that indicates complementary neuronal contributions and possible glial control, which is consistent with the current knowledge of astrocytes as the regulator and architect of neuronal processing (Eroglu and Barres, 2010; Panatier et al., 2011; Allen and Lyons, 2018; Mederos et al., 2018). Our findings demonstrated the activation of Ca^{2+} transients of cortical neurons and astrocytes during acupuncture stimulation, first observed in the activity of each cell-type, and second as a collective and coordinated phenomenon under chemogenetic inhibition. These findings provide the first *in vivo* and real-time evidence of neural activation induced by acupuncture.

Acknowledgments: *We thank Dr. Man Li (Tongji Medical College, Huazhong University of Science and Technology) for kind suggestions of the manuscript.*
Author contributions: *Study design, experiment implementation, and data analysis: KC, XYC; two-photon imaging experimental: TC; manuscript writing: LZ, XYC; manuscript editing: KC; manuscript revision: KFS, ESY, PTL; study supervision: LZ, KFS, ESY. All authors read and approved the final manuscript.*
Conflicts of interest: *The authors declare no conflicting interests.*
Editor note: KFS is an Editorial Board member of Neural Regeneration Research. He was blinded from reviewing or making decisions on the manuscript. The article was subject to the journal's standard procedures, with peer review handled independently of this Editorial Board member and their research groups.
Availability of data and materials: *All data generated or analyzed during this study are included in this published article and its supplementary information files.*

Additional files:
Additional Figure 1: *Co-localization of GCaMP6s in cortical excitatory neurons.*
Additional Figure 2: *Specific expression of GCaMP6f in astrocytes.*

References

Allen NJ, Lyons DA (2018) Glia as architects of central nervous system formation and function. Science 362:181-185.
Aronoff R, Matyas F, Mateo C, Ciron C, Schneider B, Petersen CC (2010) Long-range connectivity of mouse primary somatosensory barrel cortex. Eur J Neurosci 31:2221-2233.
Brancaccio M, Patton AP, Chesham JE, Maywood ES, Hastings MH (2017) Astrocytes control circadian timekeeping in the suprachiasmatic nucleus via glutamatergic signaling. Neuron 93:1420-1435.e5.
Bushnell MC, Duncan GH, Hofbauer RK, Ha B, Chen JI, Carrier B (1999) Pain perception: is there a role for primary somatosensory cortex? Proc Natl Acad Sci U S A 96:7705-7709.
Cichon J, Blanck TJJ, Gan WB, Yang G (2017) Activation of cortical somatostatin interneurons prevents the development of neuropathic pain. Nat Neurosci 20:1122-1132.
Eroglu C, Barres BA (2010) Regulation of synaptic connectivity by glia. Nature 468:223-231.
Goldman N, Chen M, Fujita T, Xu Q, Peng W, Liu W, Jensen TK, Pei Y, Wang F, Han X, Chen JF, Schnermann J, Takano T, Bekar L, Tieu K, Nedergaard M (2010) Adenosine A1 receptors mediate local anti-nociceptive effects of acupuncture. Nat Neurosci 13:883-888.
Haake M, Müller HH, Schade-Brittinger C, Basler HD, Schäfer H, Maier C, Endres HG, Trampisch HJ, Molsberger A (2007) German Acupuncture Trials (GERAC) for chronic low back pain: randomized, multicenter, blinded, parallel-group trial with 3 groups. Arch Intern Med 167:1892-1898.
Hinman RS, McCrory P, Pirotta M, Relf I, Forbes A, Crossley KM, Williamson E, Kyriakides M, Novy K, Metcalf BR, Harris A, Reddy P, Conaghan PG, Bennell KL (2014) Acupuncture for chronic knee pain: a randomized clinical trial. JAMA 312:1313-1322.
Holtmaat A, Bonhoeffer T, Chow DK, Chuckowree J, De Paola V, Hofer SB, Hübener M, Keck T, Knott G, Lee WC, Mostany R, Mrsic-Flogel TD, Nedivi E, Portera-Cailliau C, Svoboda K, Trachtenberg JT, Wilbrecht L (2009) Long-term, high-resolution imaging in the mouse neocortex through a chronic cranial window. Nat Protoc 4:1128-1144.
Jensen TS, Finnerup NB (2014) Allodynia and hyperalgesia in neuropathic pain: clinical manifestations and mechanisms. Lancet Neurol 13:924-935.
Kim S, Zhang X, O'Buckley SC, Cooter M, Park JJ, Nackley AG (2018) Acupuncture resolves persistent pain and neuroinflammation in a mouse model of chronic overlapping pain conditions. J Pain 19:1384.e1-1384.e14.
Liao HY, Hsieh CL, Huang CP, Lin YW (2017) Electroacupuncture attenuates CFA-induced inflammatory pain by suppressing Nav1.8 through S100B, TRPV1, opioid, and adenosine pathways in mice. Sci Rep 7:42531.
Linde K, Streng A, Jürgens S, Hoppe A, Brinkhaus B, Witt C, Wagenpfeil S, Pfaffenrath V, Hammes MG, Weidenhammer W, Willich SN, Melchart D (2005) Acupuncture for patients with migraine: a randomized controlled trial. JAMA 293:2118-2125.
Liu Y, Latremoliere A, Li X, Zhang Z, Chen M, Wang X, Fang C, Zhu J, Alexandre C, Gao Z, Chen B, Ding X, Zhou JY, Zhang Y, Chen C, Wang KH, Woolf CJ, He Z (2018) Touch and tactile neuropathic pain sensitivity are set by corticospinal projections. Nature 561:547-550.
Maeda Y, Kim H, Kettner N, Kim J, Cina S, Malatesta C, Gerber J, McManus C, Ong-Sutherland R, Mezzacappa P, Libby A, Mawla I, Morse LR, Kaptchuk TJ, Audette J, Napadow V (2017) Rewiring the primary somatosensory cortex in carpal tunnel syndrome with acupuncture. Brain 140:914-927.
Martin-Fernandez M, Jamison S, Robin LM, Zhao Z, Martin ED, Aguilar J, Benneyworth MA, Marsicano G, Araque A (2017) Synapse-specific astrocyte gating of amygdala-related behavior. Nat Neurosci 20:1540-1548.
Mederos S, González-Arias C, Perea G (2018) Astrocyte-neuron networks: a multilane highway of signaling for homeostatic brain function. Front Synaptic Neurosci 10:45.
Meier SD, Kafitz KW, Rose CR (2008) Developmental profile and mechanisms of GABA-induced calcium signaling in hippocampal astrocytes. Glia 56:1127-1137.
Orr AG, Hsiao EC, Wang MM, Ho K, Kim DH, Wang X, Guo W, Kang J, Yu GQ, Adame A, Devidze N, Dubal DB, Masliah E, Conklin BR, Mucke L (2015) Astrocytic adenosine receptor A2A and Gs-coupled signaling regulate memory. Nat Neurosci 18:423-434.
Panatier A, Vallée J, Haber M, Murai KK, Lacaille JC, Robitaille R (2011) Astrocytes are endogenous regulators of basal transmission at central synapses. Cell 146:785-798.
Park JY, Namgung U (2018) Electroacupuncture therapy in inflammation regulation: current perspectives. J Inflamm Res 11:227-237.
Percie du Sert N, Hurst V, Ahluwalia A, Alam S, Avey MT, Baker M, Browne WJ, Clark A, Cuthill IC, Dirnagl U, Emerson M, Garner P, Holgate ST, Howells DW, Karp NA, Lazic SE, Lidster K, MacCallum CJ, Macleod M, Pearl EJ, et al. (2020) The ARRIVE guidelines 2.0: Updated guidelines for reporting animal research. PLoS Biol 18:e3000410.
Rosenthal ZP, Raut RV, Bowen RM, Snyder AZ, Culver JP, Raichle ME, Lee JM (2021) Peripheral sensory stimulation elicits global slow waves by recruiting somatosensory cortex bilaterally. Proc Natl Acad Sci U S A 118.
Scarborough BM, Smith CB (2018) Optimal pain management for patients with cancer in the modern era. CA Cancer J Clin 68:182-196.
Schneider CA, Rasband WS, Eliceiri KW (2012) NIH Image to ImageJ: 25 years of image analysis. Nat Methods 9:671-675.
Shigetomi E, Tong X, Kwan KY, Corey DP, Khakh BS (2011) TRPA1 channels regulate astrocyte resting calcium and inhibitory synapse efficacy through GAT-3. Nat Neurosci 15:70-80.
Stobart JL, Ferrari KD, Barrett MJP, Glück C, Stobart MJ, Zuend M, Weber B (2018) Cortical circuit activity evokes rapid astrocyte calcium signals on a similar timescale to neurons. Neuron 98:726-735.e4.
Torres-Rosas R, Yehia G, Peña G, Mishra P, del Rocio Thompson-Bonilla M, Moreno-Eutimio MA, Arriaga-Pizano LA, Isibasi A, Ulloa L (2014) Dopamine mediates vagal modulation of the immune system by electroacupuncture. Nat Med 20:291-295.
Walker EM, Rodriguez AI, Kohn B, Ball RM, Pegg J, Pocock JR, Nunez R, Peterson E, Jakary S, Levine RA (2010) Acupuncture versus venlafaxine for the management of vasomotor symptoms in patients with hormone receptor-positive breast cancer: a randomized controlled trial. J Clin Oncol 28:634-640.
Witt C, Brinkhaus B, Jena S, Linde K, Streng A, Wagenpfeil S, Hummelsberger J, Walther HU, Melchart D, Willich SN (2005) Acupuncture in patients with osteoarthritis of the knee: a randomised trial. Lancet 366:136-143.
Yu X, Nagai J, Khakh BS (2020) Improved tools to study astrocytes. Nat Rev Neurosci 21:121-138.

C-Editor: Zhao M; S-Editors: Yu J, Li CH; L-Editors: McCollum L, Yu J, Song LP; T-Editor: Jia Y

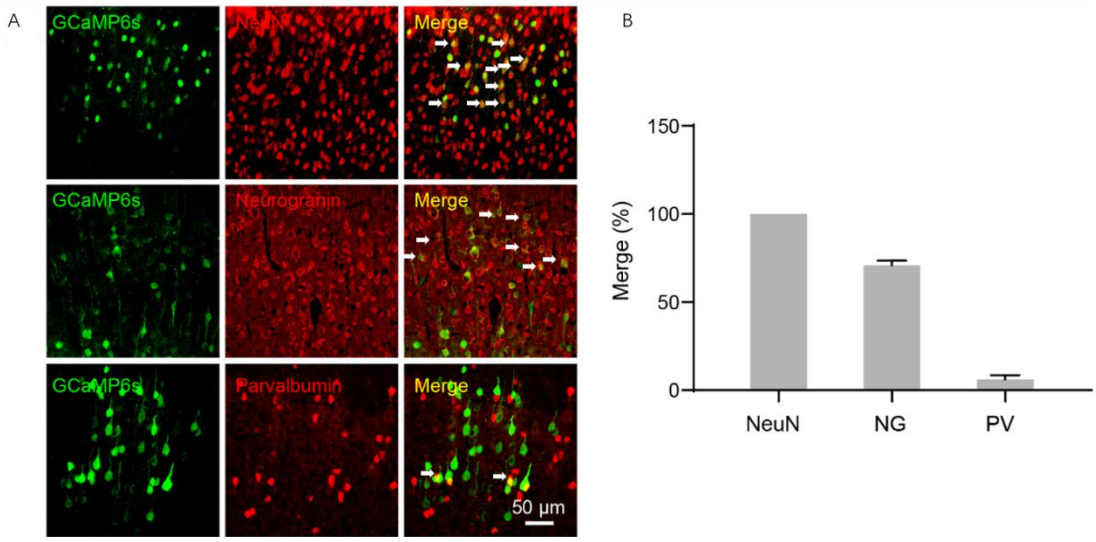

Additional Figure 1 Co-localization of GCaMP6s in cortical excitatory neurons.

(A) Immunofluorescent staining of co-localization (arrows) of GCaMP6s (green) and NeuN (red, stained by Alexa Fluor 594), Neurogranin (red, stained by Alexa Fluor 594) or parvalbumin (red, stained by Alexa Fluor 594). A higher co-localization ratio of GCaMP6s in excitatory (Neurogranin, NG) neurons but not in GABAergic parvalbumin (PV) cells. Scale bar: 50 μm. (B) Percentage of co-localization of GCaMP6s and NeuN, Neurogranin or parvalbumin. Data are expressed as mean ± SEM. The experiments were repeated twice. GCaMP6s: green fluorescent-calmodulin proteins.

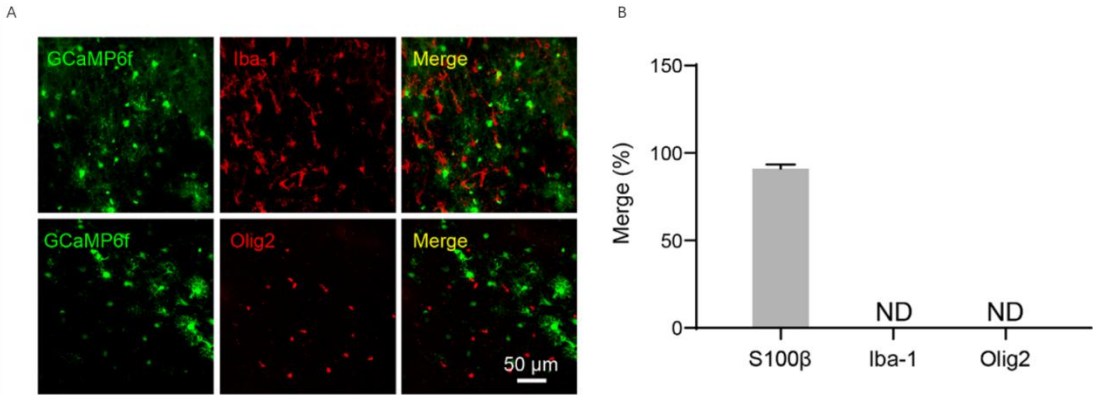

Additional Figure 2 Specific expression of GCaMP6f in astrocytes.

(A) Immunofluorescent staining of co-localization of GCaMP6s (green) and S100β (red, stained by Alexa Fluor 594), Iba-1 (red, stained by Alexa Fluor 594) or Olig2 (red, stained by Alexa Fluor 594). GCaMP6f under the driven of gfaABC1D promoter was mainly expressed in astrocytes (S100β) but not microglia (Iba-1) or oligodendrocytes (Olig2). Scale bar: 50 μm. (B) Percentage of co-localization of GCaMP6s and S100β, NIba-1 or Olig2. Data are expressed as mean ± SEM. The experiments were repeated twice. GCaMP6s: green fluorescent-calmodulin proteins; Iba-1: ionized calcium binding adaptor molecule 1; ND: non-detectable level.